

Substorm-like aurora at Jupiter

B. Bonfond^{1*†}, Z. H. Yao^{1,2†}, G. R. Gladstone³, D. Grodent¹, J.-C. Gérard¹, J. Matar¹, T. K. Greathouse³, V. Hue³, M. H. Versteeg³, J. A. Kammer³, C. Tao⁴, M. F. Vogt⁵, A. Mura⁶, A. Adriani⁶, B. H. Mauk⁷, W. S. Kurth⁸, S. J. Bolton³

¹ Space Science, Technologies and Astrophysical Research Institute, Laboratory for Planetary and Atmospheric Physics, University of Liège, Liège, Belgium.

² Laboratory of Earth and Planetary Physics, Institute of Geology and Geophysics, Chinese Academy of Sciences, Beijing, China.

³ Southwest Research Institute, San Antonio, TX, USA.

⁴ National Institute of Information and Communications Technology, Tokyo, Japan.

⁵ Center for Space Physics, Boston University, MA, USA.

⁶ Institute for Space Astrophysics and Planetology, National Institute for Astrophysics, Rome, Italy.

⁷ Applied Physics Laboratory, Johns Hopkins University, Laurel, MD, USA.

⁸ Department of Physics and Astronomy, University of Iowa, Iowa City, IA, USA.

*Correspondence to: b.bonfond@uliege.be.

†These authors contributed equally to this work.

Polar aurorae are a direct consequence of the dynamics of the plasma in the magnetosphere. The sources of mass and energy differ between the Earth's and Jupiter's magnetospheres^{1,2}, hence leading to fundamentally distinct auroral morphologies and very different responses to solar wind variations. Here we report on the imaging of all development stages of spectacular auroral events at Jupiter, called dawn storms^{3,4}, including their initiation on the night side. Our results reveal surprising similarities with auroral substorms at Earth, which stem from explosive magnetospheric reconfigurations. These findings demonstrate that, whatever their sources, mass and energy do not always circulate smoothly in planetary magnetospheres. Instead they often accumulate until the

magnetospheres reconfigure and generate substorm-like responses in the planetary aurorae.

The specificity of the dawn storms among the various auroral morphologies at Jupiter was recognized as soon as the first high resolution ultraviolet (UV) images of the aurorae on Jupiter became available³. As seen from the Hubble Space Telescope (HST), which has only access to the Earth-facing side of the aurora, they consist of a thickening and a major enhancement of the brightness of the dawn arc of the main auroral emission (main oval). They seem to last at least for 1-2 hours⁴ while the typical length of HST sequences is ~45 minutes, therefore they could not provide a complete view of the process. Dawn storms are also characterized by very clear signatures of methane absorption, indicating that the charged particles causing them can precipitate deep below the methane homopause, with energies up to 460 keV⁵ in the case of electrons. Based on the large HST observation campaign carried out in 2007, dawn storms appeared rare (3 cases out of 54 observations) and occurred indifferently to the state of the solar wind⁶. However, the dawn storm observed during the HST campaign supporting the Juno mission as it approached Jupiter in 2016 occurred just as a coronal mass ejection hit Jupiter's magnetosphere, re-igniting the debate on the relationship between dawn storms and solar wind fluctuations. So far, our understanding of dawn storms has been incomplete mainly because we have been unable to observe the whole extent of the event, both temporally and spatially. New data from the Juno mission reveal for the first time where and how the dawn storms start and the consequences to which they lead.

Juno is a NASA New Frontiers spacecraft orbiting Jupiter since July 4th 2016. Its 53-day eccentric polar orbit brings its perijove (PJ) to ~4000 km high above the surface (1 bar level) at the equator. This orbit allows its ultraviolet spectrograph (UVS) to acquire spectrally resolved

images of the northern and then the southern polar aurorae during a time interval approximately comprised between 4 hours before and 4 hours after the PJ. The spin-stabilized spacecraft rotates every 30s and the UVS scan mirror allows UVS to point the 7.2° long slit up to 30° away from the spin plane in each direction⁷. Since UVS cannot observe the whole aurora during a given spin during the perijove sequence, the exact timing of some transient events is uncertain.

For the first time, Juno-UVS has granted us a complete and global picture of the auroral dawn storms, from their initiation to their vanishing. Indeed, Juno captured views of dawn storms at different stages of development in approximately half of the perijoves performed to date (Table 1).

For example, on 7 February 2018 (PJ11), Juno-UVS captured the initiation of a dawn storm at low altitude (~43000 km) over the north pole, thus allowing unprecedented high spatial resolution observations (Figure 1). Around 13:06 UT, the event started with a relatively bright midnight arc (~2000 kR). Then a few north-south aligned elongated spots began to appear poleward of this arc, forming a string of approximately a dozen spots within 15 minutes, each one bursting dusk-ward of the previous. Using the flux mapping method of Vogt et al. [2015]⁸, but with JRM09⁹ as an internal field model, these spots map to a distance of 110-125 Jovian radii and a local time range between 22:40 UT and 23:20 UT, which broadly corresponds to the X-line, where magnetotail reconnections take place¹⁰. Even though the spin modulated sampling rate of UVS does not allow for easy tracking of their motion, individual spots appear to move equatorward before vanishing after a few minutes.

Two hours later, Juno was located in the southern hemisphere when the main emission began to brighten and broaden irregularly, forming a bead-like pattern in the same midnight sector. Flybys carried out at lower altitude during this phase of the dawn storm, such as during PJ3 at 15:37

UT, render this pattern, with beads with ~ 1500 km ($\sim 2^\circ$) spacing, even more obvious. Hence, the enhancement of the main emission, leading to the full-fledged dawn storm, actually started around midnight. This feature then slowly migrated to the dawn sector at a pace corresponding to $\sim 25\%$ of the corotation with the planet. Around 16:22 UT, the main arc split into two parts, one moving towards the pole and the other moving equatorward. The whole feature continued to rotate, progressively accelerating towards co-rotation with the magnetic field as the dawn storm developed. Juno flew away from the planet and the UVS observations ended at 18:50 UT, while the event was still ongoing.

On 19 May 2017 (PJ6), the Juno-UVS observations missed the beginning of the event, but they allowed us to examine the next phases. After the broadening and the splitting of the main emission, the outer arc transformed into large blobs. On the same day, subsequent HST images acquired with the Space Telescope Imaging Spectrograph (STIS) confirmed that the blobs continued their evolution, forming latitudinally extended fingers slowly expanding equatorward. Such features have been associated with large and fresh plasma injection signatures¹¹. While such a connection between dawn storms and large injection signatures has been proposed previously¹², this long and continuous set of observations is the first to clearly demonstrate one changing into the other. It should also be noted that some (but less intense) injection signatures can also appear independently from dawn storms¹³.

Put together, the Juno-UVS observations from PJ11 and PJ6 paint a brand new picture of the dawn storms, as it consists of a 5-10 hours long chain of events, starting with the transient elongated spots, followed a few hours later by the formation of bead-like features on the midnight part of the main emissions. Then follows an expansion phase, during which the main emission brightens, expands, thickens and forks into two branches migrating poleward and

equatorward respectively. This chain of events is very similar to the one observed during terrestrial auroral substorms (Fig. 2). Substorms are global reconfigurations of the magnetosphere during which the magnetic energy stored in the magnetotail is converted into particle energy, which lead to spectacular auroral brightening in nightside polar region which generally follow a well-established sequence of features¹⁴. The transient elongated spots look like similar transient and north-south aligned spots on Earth, sometimes associated with poleward boundary intensifications¹⁵ and sometimes with streamers, which are both observed before the substorm onset¹⁶. Both phenomena are associated with reconnection in the magnetotail and the subsequent inward flow of plasma and dipolarizing field lines¹⁷. The pre-expansion beads observed in the context of terrestrial substorms are associated with plasma instabilities in the near magnetotail, such as the ballooning instability¹⁸. The expansion phases of dawn storms and substorms are also very similar, and the later corresponds to a dipolarization/current disruption in the magnetosphere. Finally, the auroral blobs in the equatorward emissions manifest massive plasma injections. While plasma injections in the inner terrestrial magnetosphere do not generally induce distinct auroral emission, they are indeed observed by in-situ instruments during substorm events¹⁹. One notable difference is that auroral substorms do not rotate with the Earth, but evolve in fixed local time, i.e., around midnight.

At Earth, substorms do not always occur as isolated events, instead multiple substorm expansions can happen consecutively²⁰. A similar behavior is observed for dawn storms at Jupiter. For example, on 27 March 2017 (PJ5), a first dawn storm was ongoing when the observations started at 03:57 UT and was finished by approximately 06:51 UT while a second one was observed peaking around 08:14 UT (Fig. 3). During PJ3, the dawn storm expansion phase seemed to never really stop, continuously going on at the same local time. Again, such a

behavior is not uncommon for terrestrial substorms. The occurrence of successive dawn storms separated by a delay of a few hours could explain why images of dawn storms from HST often display large injection signatures in the post-noon sector^{12,21}.

Terrestrial substorms vary considerably in intensity and those which could not fully develop are called pseudo-breakups²². The event observed during PJ16 (29 October 2018) was limited to a small intensification, which might be analogous to terrestrial pseudo-breakups (Fig. S2). Around 20:19 UT, Juno-UVS captured the appearance of three transient (~6 minutes) and elongated spots poleward of the midnight arc of the main emission. Moreover, the midnight arc itself was fainter than during PJ11 and the number of spots was also lower. The enhancement of the dawn arc of the main emission observed at 23:39 UT was a fairly dim (~500 kR), as was the area concerned with the enhancement (~10° in longitude). While the sequence of events is similar to the one observed on PJ11, which is why we identify it here as a dawn storm, it probably would not have been qualified as a dawn storm in previous studies, due to its limited extent and brightness. This and the fact that Juno observes the whole auroral region, including the night side where dawn storms arise, almost continuously for ~8 hours explains the discrepancy between our detection rate and the one deduced from HST, which only focused on the expansion phase. The second dawn storm on PJ5 is another example of a limited dawn storm.

The orientation and strength of the solar wind control the occurrence and intensity of Earth substorms²³, but these parameters cannot be measured at Jupiter while Juno carries out its perijove observations. Instead, we used the propagation model from Tao et al. [2005]²⁴, which relies on measurements acquired at one astronomical unit (from either the OMNI data or the Stereo A spacecraft) to estimate the solar wind velocity and dynamic pressure at Jupiter when Jupiter and the observatory are sufficiently well aligned (<40°) (Figs. S3-S5). Most dawn storms

for which such an estimate was possible (i.e. PJ5, PJ9, PJ14 and PJ20) happened more than 2 days away from any solar wind enhancements, which confirms that dawn storm occur during relaxed solar wind conditions. However, they can also occur at times closer to a solar wind enhancement (e.g. PJ1, PJ6 and PJ16), suggesting that solar wind shocks do not necessarily prevent their occurrence.

Regardless of the similarities between terrestrial substorms and jovian dawn storms, it is also important to stress the major differences between the Earth's and Jupiter's magnetospheres²⁵.

The first is dominated by its interaction with the solar wind, and magnetic reconnections on the dayside magnetopause drive the plasma convection in the magnetosphere through the so-called Dungey cycle¹. On the other hand, the Jovian magnetosphere is inflated with plasma originating from the volcanic moon Io and the rotation of the planet controls the motion and the energization of the magnetospheric plasma. The mechanism through which the mass injected at Io is ultimately released via reconnection on closed field lines is called the Vasyliunas cycle².

However, regardless of the different reasons for the loading, in both cases plasma and energy regularly accumulates within the system, which grows increasingly unstable, especially in the midnight magnetotail where the field lines are the most elongated. Such a stretching of the field lines provides favorable conditions for reconnection to occur. At Earth, such reconnection closes the magnetic field lines open to the solar wind in the magnetotail, while at Jupiter, reconnection is internally driven^{26–28} and is expected to take place on closed field lines. In the middle magnetosphere, various plasma instabilities may occur, such as ballooning instability²⁹ or cross-field current instability³⁰. Since the magnetic field lines in Jupiter's outer magnetosphere are also highly stretched, and the magnetosphere consists of more energetic ions than the Earth's magnetotail, many plasma instabilities identified in Earth's magnetotail would likely take place

in Jupiter's outer magnetosphere. Such instabilities can then lead to a disruption of the azimuthal currents in the middle magnetosphere and a depolarization of the field lines. While the dipolarizing field lines would remain in the night sector at Earth, they would be progressively swept away by the planetary rotation at Jupiter as they progress inward. These processes would also bring hot and sparse plasma from the outer magnetosphere further into the system and energize it, forming plasma injections. Even if the overall dynamics of the plasma in the two magnetospheres are fundamentally different, one being externally driven and the other being internally driven, universal processes releasing the accumulated matter and energy from the systems lead to strikingly similar auroral signature.

References and Notes:

1. Dungey, J. W. Interplanetary Magnetic Field and the Auroral Zones. *Phys. Rev. Lett.* **6**, 47–48 (1961).
2. Vasyliunas, V. M. Physics of the Jovian magnetosphere. in *Physics of the Jovian Magnetosphere* (ed. Dessler, A. J.) 395–453 (Cambridge University Press, 1983).
3. Gérard, J. C. *et al.* A Remarkable Auroral Event on Jupiter Observed in the Ultraviolet with the Hubble Space Telescope. *Science* **266**, 1675–1678 (1994).
4. Ballester, G. E. *et al.* Time-Resolved Observations of Jupiter's Far-Ultraviolet Aurora. *Science* **274**, 409–413 (1996).
5. Gustin, J. *et al.* Characteristics of Jovian morning bright FUV aurora from Hubble Space Telescope/Space Telescope Imaging Spectrograph imaging and spectral observations. *Journal of Geophysical Research: Space Physics* **111**, (2006).

6. Nichols, J. D., Clarke, J. T., Gérard, J. C., Grodent, D. & Hansen, K. C. Variation of different components of Jupiter's auroral emission. *Journal of Geophysical Research (Space Physics)* **114**, A06210 (2009).
7. Gladstone, G. R. *et al.* The Ultraviolet Spectrograph on NASA's Juno Mission. *Space Sci Rev* **213**, 447–473 (2017).
8. Vogt, M. F. *et al.* Magnetosphere-ionosphere mapping at Jupiter: Quantifying the effects of using different internal field models. *Journal of Geophysical Research: Space Physics* **120**, 2584–2599 (2015).
9. Connerney, J. E. P. *et al.* A New Model of Jupiter's Magnetic Field From Juno's First Nine Orbits. *Geophysical Research Letters* **45**, 2590–2596 (2018).
10. Vogt, M. F., Kivelson, M. G., Khurana, K. K., Joy, S. P. & Walker, R. J. Reconnection and flows in the Jovian magnetotail as inferred from magnetometer observations. *Journal of Geophysical Research: Space Physics* **115**, (2010).
11. Dumont, M. *et al.* Evolution of the Auroral Signatures of Jupiter's Magnetospheric Injections. *Journal of Geophysical Research: Space Physics* **0**, (2018).
12. Gray, R. L. *et al.* Auroral evidence of radial transport at Jupiter during January 2014. *Journal of Geophysical Research: Space Physics* **121**, 9972–9984 (2016).
13. Bonfond, B. *et al.* Morphology of the UV aurorae Jupiter during Juno's first perijove observations. *Geophysical Research Letters* **44**, 4463–4471 (2017).
14. Akasofu, S.-I. Auroral Morphology: A Historical Account and Major Auroral Features During Auroral Substorms. in *Auroral Phenomenology and Magnetospheric Processes: Earth And Other Planets* 29–38 (American Geophysical Union (AGU), 2013).
doi:10.1029/2011GM001156.

15. Nishimura, Y., Lyons, L., Zou, S., Angelopoulos, V. & Mende, S. Substorm triggering by new plasma intrusion: THEMIS all-sky imager observations. *Journal of Geophysical Research: Space Physics* **115**, (2010).
16. Nishimura, Y. *et al.* Relations between multiple auroral streamers, pre-onset thin arc formation, and substorm auroral onset. *Journal of Geophysical Research: Space Physics* **116**, (2011).
17. Angelopoulos, V. *et al.* Tail Reconnection Triggering Substorm Onset. *Science* **321**, 931–935 (2008).
18. Yao, Z., Pu, Z. Y., Rae, I. J., Radioti, A. & Kubyshkina, M. V. Auroral streamer and its role in driving wave-like pre-onset aurora. *Geoscience Letters* **4**, 8 (2017).
19. Gabrielse, C. *et al.* Utilizing the Heliophysics/Geospace System Observatory to Understand Particle Injections: Their Scale Sizes and Propagation Directions. *Journal of Geophysical Research: Space Physics* **124**, 5584–5609 (2019).
20. Liou, K., Newell, P. T., Zhang, Y.-L. & Paxton, L. J. Statistical comparison of isolated and non-isolated auroral substorms. *Journal of Geophysical Research: Space Physics* **118**, 2466–2477 (2013).
21. Grodent, D. *et al.* Jupiter’s Aurora Observed With HST During Juno Orbits 3 to 7. *Journal of Geophysical Research: Space Physics* **123**, 3299–3319 (2018).
22. Pulkkinen, T. I. *et al.* Pseudobreakup and substorm onset: Observations and MHD simulations compared. *Journal of Geophysical Research: Space Physics* **103**, 14847–14854 (1998).
23. Kullen, A. & Karlsson, T. On the relation between solar wind, pseudobreakups, and substorms. *Journal of Geophysical Research: Space Physics* **109**, (2004).

24. Tao, C., Kataoka, R., Fukunishi, H., Takahashi, Y. & Yokoyama, T. Magnetic field variations in the Jovian magnetotail induced by solar wind dynamic pressure enhancements. *Journal of Geophysical Research: Space Physics* **110**, (2005).
25. Mauk, B. & Bagenal, F. Comparative Auroral Physics: Earth and Other Planets. in *Auroral Phenomenology and Magnetospheric Processes: Earth And Other Planets* 3–26 (American Geophysical Union (AGU), 2013). doi:10.1029/2011GM001192.
26. Kronberg, E. A. *et al.* Mass release at Jupiter: Substorm-like processes in the Jovian magnetotail. *Journal of Geophysical Research: Space Physics* **110**, (2005).
27. Woch, J., Krupp, N. & Lagg, A. Particle bursts in the Jovian magnetosphere: Evidence for a near-Jupiter neutral line. *Geophysical Research Letters* **29**, 42-1-42–4 (2002).
28. Ge, Y. S., Russell, C. T. & Khurana, K. K. Reconnection sites in Jupiter’s magnetotail and relation to Jovian auroras. *Planetary and Space Science* **58**, 1455–1469 (2010).
29. Hameiri, E., Laurence, P. & Mond, M. The ballooning instability in space plasmas. *Journal of Geophysical Research: Space Physics* **96**, 1513–1526 (1991).
30. Lui, A. T. Y., Chang, C.-L., Mankofsky, A., Wong, H.-K. & Winske, D. A cross-field current instability for substorm expansions. *Journal of Geophysical Research: Space Physics* **96**, 11389–11401 (1991).
31. Adriani, A. *et al.* JIRAM, the Jovian Infrared Auroral Mapper. *Space Sci Rev* **213**, 393–446 (2017).
32. T. K. Greathouse, G. R. Gladstone, M. W. Davis, D. C. Slater, M. H. Versteeg, K. B. Persson, B. C. Walther, G. S. Winters, S. C. Persyn, J. S. Eterno, in UV, X-Ray, and Gamma-Ray Space Instrumentation for Astronomy XVIII (International Society for Optics and Photonics, 2013; <https://www.spiedigitallibrary.org/conference-proceedings-of->

spie/8859/88590T/Performance-results-from-in-flight-commissioning-of-the-Juno-Ultraviolet/10.1117/12.2024537.short), vol. 8859, p. 88590T.

33. V. Hue, J. Kammer, G. R. Gladstone, T. K. Greathouse, M. W. Davis, B. Bonfond, M. H. Versteeg, D. Grodent, J.-C. Gérard, S. J. Bolton, S. M. Levin, in Space Telescopes and Instrumentation 2018: Ultraviolet to Gamma Ray (International Society for Optics and Photonics, 2018; <https://www.spiedigitallibrary.org/conference-proceedings-of-spie/10699/1069931/In-flight-characterization-and-calibration-of-the-Juno-Ultraviolet-Spectrograph/10.1117/12.2311563.short>), vol. 10699, p. 1069931.

34. A. Mura, A. Adriani, F. Altieri, J. E. P. Connerney, S. J. Bolton, M. L. Moriconi, J.-C. Gérard, W. S. Kurth, B. M. Dinelli, F. Fabiano, F. Tosi, S. K. Atreya, F. Bagenal, G. R. Gladstone, C. Hansen, S. M. Levin, B. H. Mauk, D. J. McComas, G. Sindoni, G. Filacchione, A. Migliorini, D. Grassi, G. Piccioni, R. Noschese, A. Cicchetti, D. Turrini, S. Stefani, M. Amoroso, A. Olivieri, Infrared observations of Jovian aurora from Juno's first orbits: Main oval and satellite footprints. *Geophysical Research Letters*. 44, 5308–5316 (2017).

Acknowledgments: The authors are grateful to J.E.P. Connerney for helpful discussions concerning the manuscript. **Funding:** B.B. is a Research Associate of the Fonds de la Recherche Scientifique - FNRS. We are grateful to NASA and contributing institutions which have made the Juno mission possible. This work was funded by NASA's New Frontiers Program for Juno via contract with the Southwest Research Institute. B.B., D.G., J.-C.G., and J.M. acknowledge financial support from the Belgian Federal Science Policy Office (BELSPO) via the PRODEX Programme of ESA. The research at the University of Iowa was supported by NASA through Contract 699041X with Southwest Research Institute; **Author contributions:** Preparation of the manuscript, figures, calculations, data analysis was performed by B.B and Z.Y.; additional help for the production of several figures by J.M. and A.M.; data interpretation was performed by B.B., Z.Y., D.G., C.T. and A.M.; revisions of the manuscript were made by B.B., Z.Y., G.G., D.G., J.-C.G., J.M., T.G., V.H., C.T., M.Vo. and W.K.; S.B. is the Juno principal investigator;

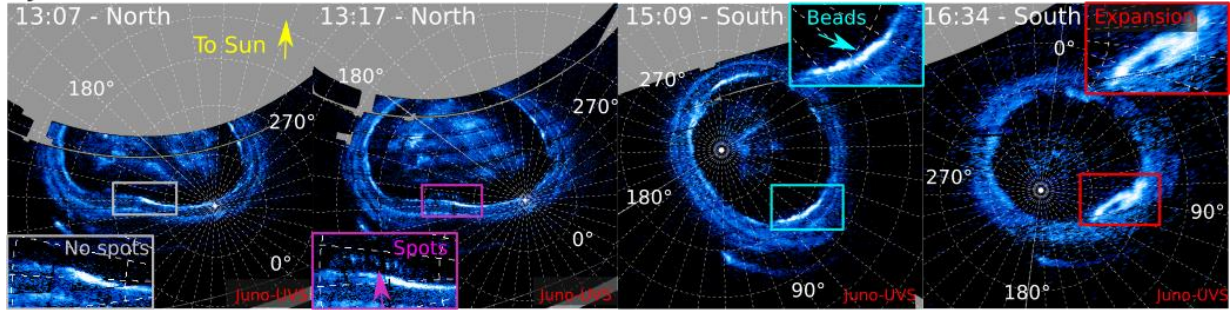
G.G. is responsible for the UVS instrument; A.A. is responsible for the JIRAM instrument; D.G. is the principal investigator of the G14634 HST campaign; modeling of the solar wind propagation by C.T.; modeling of the Jovian magnetic field mapping by M.Vo.; preparation for measurements and data acquisition was performed by G.G., V.H., T.G., M.Ve., J.K. and B.B.; calibration was done by G.G., V.H., T.G. and J.K.; **Competing interests:** Authors declare no competing interest; and **Data and materials availability:** The data included herein are either archived or on schedule to be archived in NASA's Planetary Data System (http://pds-atmospheres.nmsu.edu/data_and_services/atmospheres_data/JUNO/juno.html). This research is also based on publicly available observations acquired with the NASA/ESA Hubble Space Telescope and obtained at the Space Telescope Science Institute, which is operated by AURA for NASA (<https://archive.stsci.edu/hst/search.php>). Data analysis was performed with the AMDA science analysis system provided by the Centre de Données de la Physique des Plasmas (CDPP) supported by CNRS, CNES, Observatoire de Paris and Université Paul Sabatier, Toulouse. The THEMIS data are available from <http://themis.ssl.berkeley.edu/data/themis/>. The IMAGE-WIC images can be accessed at <https://spdf.gsfc.nasa.gov/pub/data/image/fuv/> and were processed using the FUVIEW3 software (<http://sprg.ssl.berkeley.edu/image/>).

Supplementary Materials:

Materials and Methods

Figures S1-S5

PJ11



PJ6

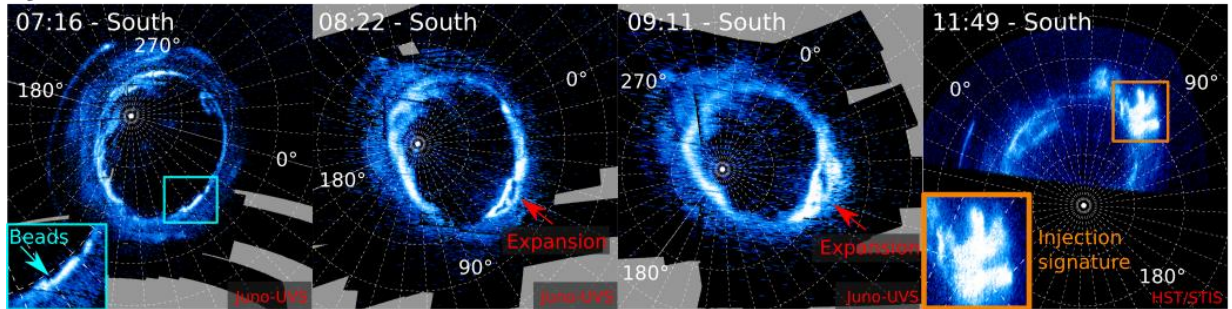


Fig. 1. Polar projection of the development of a dawn storm, based on observations acquired by Juno-UVS and HST/STIS during the 11th and the 6th perijove sequences. On PJ11, the event was preceded by the progressive appearance of a set of transient elongated spots poleward of the main emission. Two hours later, the dawn storm itself started as an enhancement of the main emission in the form of beads before the arc began to fork and expand, both latitudinally and longitudinally. On the PJ6 sequence, the same sequence of emergence of beads, followed by the expansion phase is observed, but subsequent observations by both Juno-UVS and HST-STIS show that the equatorward arc transforms into a large injection signature.

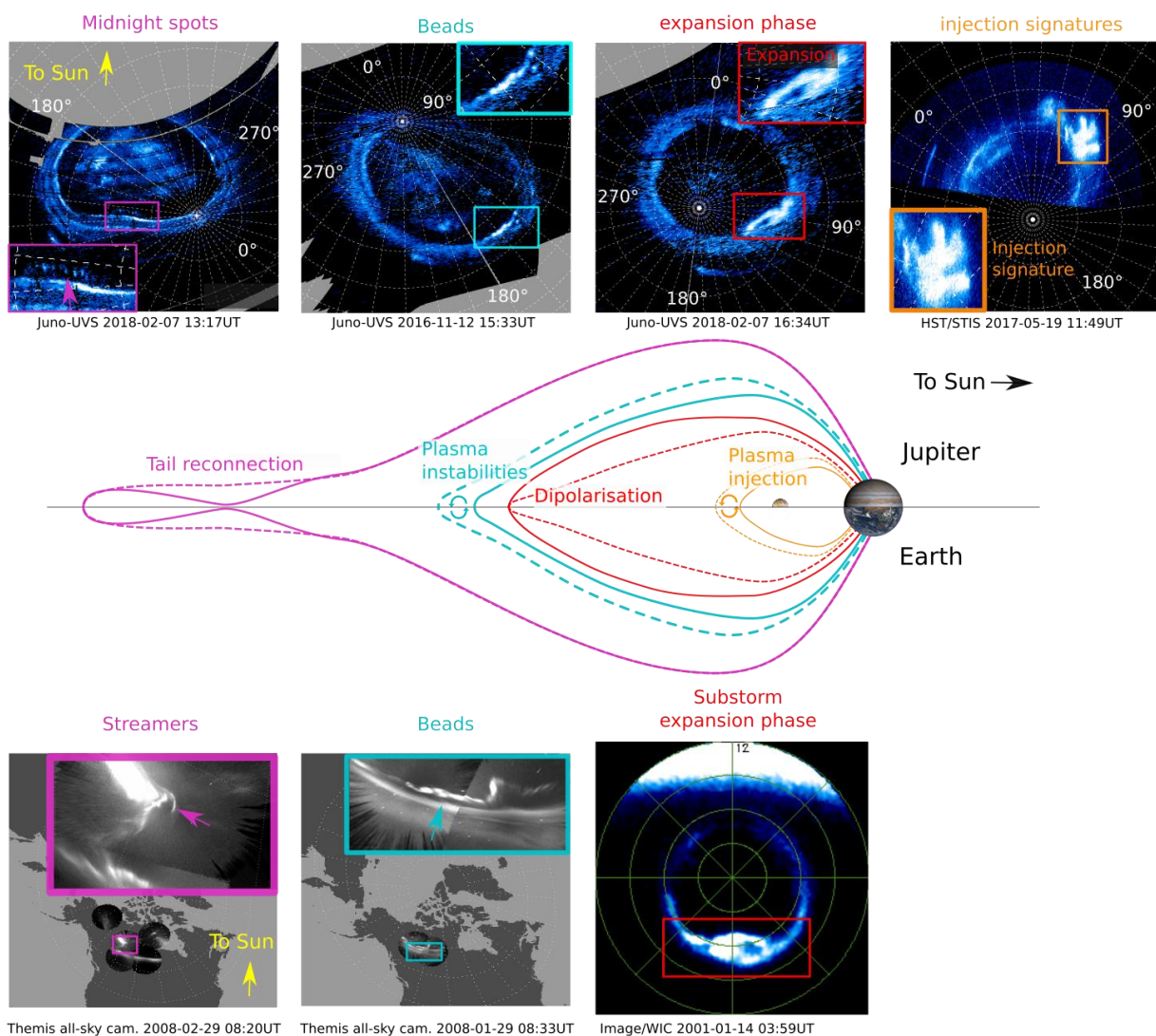


Fig. 2. Polar projections of the UV aurora showing four different phases of a Jovian dawn storm: 1) the short lived polar midnight spots, 2) the formation of irregularities on the main emission pre-dawn part 3) the expansion phase, with the two arcs splitting and 4) the injection signatures in the outer emission. The first three images are based on data from the Juno-UVS instrument and the fourth one comes from Hubble Space Telescope observations carried out to support Juno. These four phases appear to correspond to night-side tail reconnection, plasma instabilities, current disruption/dipolarization in the middle magnetosphere and to flux tube interchange, respectively, as illustrated in the general scheme shown in the central scheme (not to scale). These auroral features corresponding to these phases in the terrestrial aurora are shown on the bottom row. In the bottom, the first two images come from the THEMIS network of all-sky cameras^{15,18}. The third image corresponds to Earth's aurora as seen from IMAGE-WIC.

Non-Isolated Dawn Storms

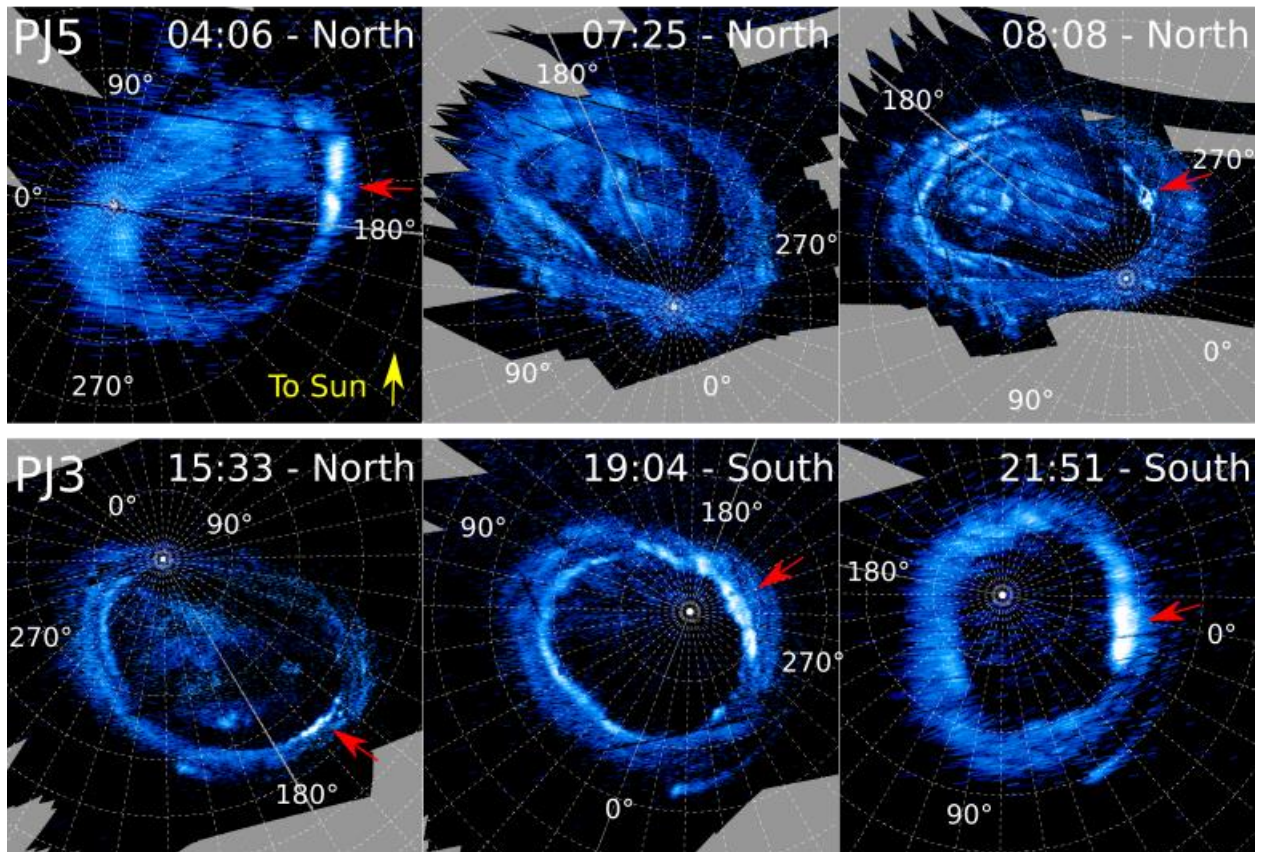


Fig. 3. Polar projections of the development of non-isolated dawn storms during PJ3 and PJ5. The red arrow highlights the dawn storms. During PJ5, a second dawn storm took place ~3 hours after the first one. On PJ3, new dawn storms seem to appear during all the southern branch of the perijove sequence.

	date	Peak power (W)	Identified features
PJ1	27 Aug 2016 18:00 => 20:00		b, e
PJ3	11 Dec 2016 15:10 => 22:02	$8.1 \cdot 10^{11}$	b, e, nids
PJ5	27 Mar 2017 3:56 => 06:00 7 :33=> 11 :09	$1.5 \cdot 10^{11}$ $1.1 \cdot 10^{11}$	b,e, nids
PJ6	19 May 2017 07:14 => 10:54	$1.6 \cdot 10^{12}$	b,e, i
PJ7	10 Jul 2017 22:43 => 00:00	$2.7 \cdot 10^{11}$	e, i
PJ9	24 Oct 2017 12:19 => 13:50	$6.0 \cdot 10^{11}$	e
PJ11	07 Feb 2018 12:58 => 18:49	$8.5 \cdot 10^{11}$	s, b, e
PJ14	16 Jul 2018 08:42=> 10:15	$6.5 \cdot 10^{11}$	e
PJ16	29 Oct 2018 23:20=> 01:00	$1.4 \cdot 10^{11}$	s, b, i
PJ20	29 May 2019 09 :30 => 12 :54	$9.2 \cdot 10^{11}$	b, e, i

Table 1. List of the dawn storms identified during Juno's perijove observations sequences. The first column collects the approximate times of the expansion phases of the dawn storm. The end time in particular are approximate, as there is no clear criterion for when the phenomenon is really finished. Start and end times in bold indicate that the observations started or ended at the indicated time, but the dawn storm probably lasted longer. The second column indicate the peak power reached by the dawn storm and the third column indicates the observed feature during this sequence, (s) meaning the spots, (b) the beads, (e) the expansion, (i) the injections and (nids) the occurrence of non-isolated dawn storms. The PJ1 dawn storm started after the end of the UVS observations, but the beginning of the expansion phase was observed with the JIRAM (Jovian InfraRed Auroral Mapper) instrument ³¹ (Fig. S1).